Journal of Metals, Materials and Minerals, 35(4), e2389, 2025

Optically stimulated luminescence dating using the quartz inclusion method of earthenware from the Nam Tok Khao Pang archaeological site, Kanchanaburi, Thailand

Thananan PHETKONGTONG[1], Peerasak KLUBKET[2], Santi PAILOPLEE[2], Pichet LIMSUWAN[3], Akapong PHUNPUEOK[1], and Voranuch THONGPOOL[1,*]

[1] *Division of Physics, Faculty of Science and Technology, Rajamangala University of Technology Thanyaburi, Pathum Thani 12110, Thailand*
[2] *Department of Geology, Faculty of Science, Chulalongkorn University, Bangkok 10330, Thailand*
[3] *Department of Physics, Faculty of Science, King Mongkut's Institute of Technology Ladkrabang, Bangkok 10520, Thailand*

***Corresponding author e-mail**: voranut_t@rmutt.ac.th

Received date:
1 May 2025
Revised date:
21 May 2025
Accepted date:
10 June 2025

Keywords:
Optically stimulated luminescence dating;
Accumulated dose;
Single aliquot regeneration protocol;
Annual dose;
Late Neolithic

Abstract

The Nam Tok Khao Pang archaeological site, located in Tha Sao subdistrict, Sai Yok district, Kanchanaburi province, Thailand, is a limestone cave where numerous artifacts, including black-burnished earthenware fragments with in-curving rims, out-curving rims, and carinated bodies, have been discovered. Mineralogical and microstructural analyses using X-ray diffraction (XRD), energy-dispersive X-ray spectroscopy (EDS), and scanning electron microscopy (SEM) identified quartz (SiO_2) as the dominant mineral phase within a partially sintered silicate matrix. The absence of vitrification and the presence of mineral impurities indicate that the earthenware was fired at temperatures between 900°C and 1000°C. To determine the age of these ceramics, optically stimulated luminescence (OSL) dating was conducted on three black-burnished earthenware fragments using the quartz inclusion method and the single aliquot regeneration (SAR) protocol. Annual dose rates were estimated from uranium (U), thorium (Th), and potassium (K) concentrations measured by laser ablation–inductively coupled plasma mass spectrometry (LA-ICP-MS). The individual OSL ages obtained were 3.591 ± 0.63 ka, 3.479 ± 0.74 ka, and 3.717 ± 0.73 ka, yielding an average age of approximately 3.59 ± 0.34 ka. This places the artifacts within the Late Neolithic to Middle–Late Bronze Age period. These findings are consistent with the typological characteristics of the earthenware and align with radiocarbon dates obtained from charcoal collected from black-burnished earthenware vessels at the Ban Kao site, which also fall within the Late Neolithic period. This correlation supports the chronological framework of prehistoric settlement in the region and highlights the reliability of OSL dating for ceramic artifacts in tropical archaeological contexts.

1. Introduction

Kanchanaburi province, in western Thailand, is one of the most archaeologically and historically important regions in the country. Located near the Khwae Yai River and the Tha Hin Mountains, the area served as a strategic corridor linking the Central Plains of Southeast Asia with the western highlands. Its geographic position, rich natural resources, and ecological diversity made it an ideal habitat and migration route for prehistoric human groups.

Archaeological investigations in Kanchanaburi began in 1943 during World War II, when Dr. Hendrik Robert Van Heekeren, a Dutch prisoner of war conscripted to help build the Death Railway, discovered flaked stone tools and polished stone axes in gravel layers between Wang Takhian and Ban Kao stations. In 1956, Dr. Karl G. Heider unearthed numerous stone tools along the Khwae Noi River in Ban Kao subdistrict, on land owned by Mr. Lue and Mr. Bang Lueangdaeng. This discovery initiated the Ban Kao archaeological site, initially called the "Bang Site." These findings led to the Thai–Danish Prehistoric Expedition (1960 to 1962), the first collaborative excavation between Thai and foreign archaeologists. Ban Kao became the first officially mapped archaeological site in Kanchanaburi and marked the beginning of systematic archaeological research in Thailand [1].

Evidence of early settlement at the Ban Kao archaeological site highlights its importance as a key representative of prehistoric culture dating to the Neolithic and Bronze Age periods, approximately 3,000 to 4,000 years ago [2]. Artifacts from Ban Kao include polished stone tools, human remains, and a wide array of earthenware vessels—such as three-legged pots, pedestal containers, long-necked jars, and deep-bottomed trays. Most earthenware exhibits a black or dark gray hue due to a smoke-firing technique and is polished to enhance water resistance and durability. This smoke-blackened, glossy finish is a hallmark of Ban Kao ceramics. These vessels are frequently found in burial contexts, accompanied by stone tools and ornaments made of bone, shell, and stone, indicating their dual use in daily life and ritual practices associated with death and the afterlife [3].

Black-burnished earthenware from Ban Kao is characterized by its smooth, dark surface finish and distinct morphological traits such as in-curving and out-curving rims, as well as sharply defined carinated bodies. These ceramics reflect both aesthetic preferences and technological sophistication in prehistoric pottery production.

Samples of charcoal collected from black-burnished earthenware vessels at the Ban Kao site were subjected to radiocarbon dating, which determined their age to fall within the Late Neolithic period [4,5].

Interestingly, similar earthenware fragments have been found at the Nam Tok Khao Pang archaeological site, a limestone cave in Tha Sao subdistrict, Sai Yok district, Kanchanaburi province. Artifacts recovered from the cave's main chamber include various black-burnished earthenware fragments that closely resemble those from the Ban Kao cultural tradition in both form and surface treatment. This resemblance suggests cultural connections or exchange between upland communities and those in the river plains of western Thailand during the prehistoric period, around 3,000 years ago. The typological similarities between the two sites highlight the need for further study of their cultural relationships and the potential existence of a shared ceramic tradition or broader regional interaction network.

The black-burnished earthenware fragments found at the Nam Tok Khao Pang archaeological site are made from clay and have been fired using the smoking technique. Such artifacts are well-suited for dating through luminescence dating [6]. The technique of luminescence dating provides the time since minerals (e.g., quartz and feldspar) [7,8] were last heated or exposed [9] and has been widely employed in the chronological analysis of archaeological sites. Luminescence dating has been successfully applied to dating ceramic around the world [10,11]. The luminescence of ceramic dates the last exposure to heating, and the high temperature of firing ensures full zeroing. Both thermoluminescence (TL) and optically stimulated luminescence (OSL) can be used [12-14].

The key distinction between TL and OSL lies in the stimulation method used to release trapped electrons. TL requires heating the sample to high temperatures to induce luminescence, making it more suitable for fired materials such as ceramics or heated stones [15]. In contrast, OSL uses light—typically in the blue or green spectrum—to stimulate the signal, which allows for the dating of sediments and unheated materials that were last exposed to sunlight. Additionally, OSL offers improved signal stability, higher sensitivity, and the ability to isolate individual grain responses, making it preferable for many sediment dating applications [16,17].

In the present study, optically stimulated luminescence (OSL) dating was applied to black-burnished earthenware fragments from the Nam Tok Khao Pang archaeological site to address the current lack of absolute chronological data for this site. By establishing a direct and reliable age framework, the study aims to contribute to a clearer understanding of the cultural and chronological relationship between the Nam Tok Khao Pang and Ban Kao archaeological sites. The resulting OSL dates not only support the assignment of the site to the Late Neolithic to Bronze Age period but also strengthen the proposed connection between the Nam Tok Khao Pang site and the broader Ban Kao cultural complex. In addition, the elemental composition and firing temperature of the black-burnished earthenware were analyzed using X-ray diffraction (XRD), scanning electron microscopy (SEM), and energy-dispersive X-ray spectroscopy (EDS) to further characterize the technological aspects of the artifacts.

2. Experimental

2.1 Sample collection

The black-burnished earthenware fragments were collected from the Nam Tok Khao Pang Cave 2 archaeological site, which is characterized as a limestone mountain located in Tha Sao subdistrict, Sai Yok district, Kanchanaburi province. The site lies along the Tenasserim Range, a steep mountainous region extending in a north–south direction. Figure 1 presents a geographical map highlighting the study area, showing the location of Khao Pang within the mountainous terrain of Kanchanaburi province. The archaeological site, the Nam Tok Khao Pang Cave 2, is marked with a black rectangle and situated at an elevation of approximately 240 m to 480 m above sea level at the geographic coordinates 14° 16′ 31″ N, 98° 57′ 46″ E. The study area is characterized by high mountains and undulating hills, surrounded by elevations exceeding 600 m. Such a landscape is well-suited for prehistoric human settlement, particularly due to its proximity to water sources and natural caves.

The samples examined in this study are black-burnished earthenware fragments found abundantly scattered in the second chamber of the cave. Photographs of the three selected samples—K1, K2, and K3—are shown in Figure 2.

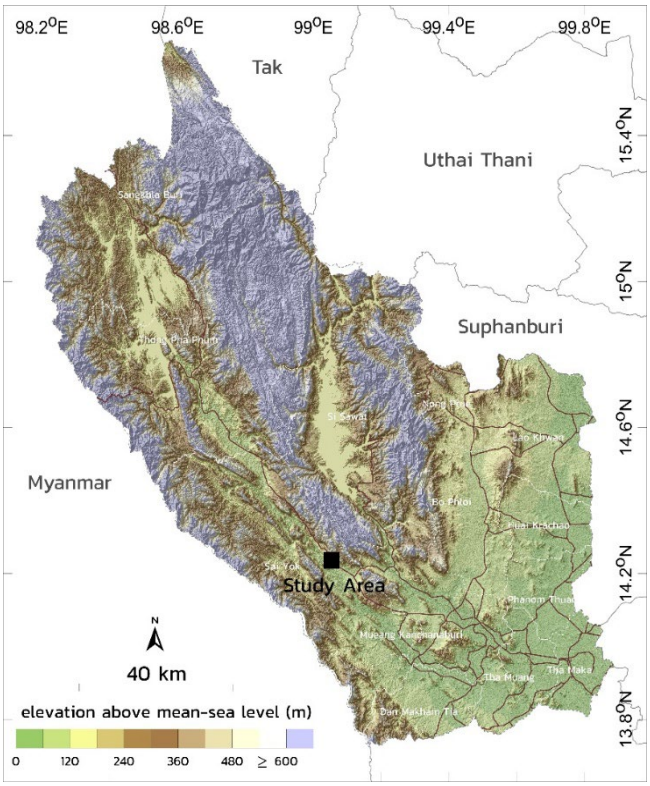

Figure 1. Study area map showing the location of Khao Pang, Kanchanaburi province.

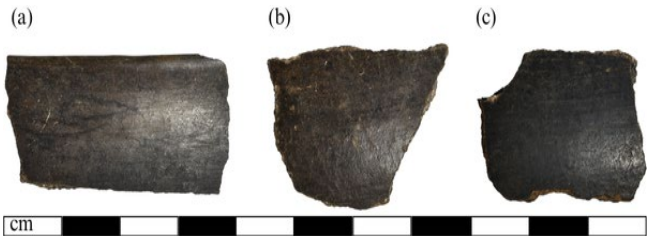

Figure 2. Photographs of the earthenware from the Nam Tok Khao Pang archaeological site (a) K1, (b) K2 and (c) K3.

2.2 Sample preparation

OSL dating was performed by calculating the ratio of the accumulated dose (AD) to the annual dose (D), where AD (measured in Gy) reflects the luminescence intensity from quartz minerals, and D (measured in Gy/a) is derived from the natural radioactivity of uranium (238U), thorium (232Th), and potassium (40K) associated with the sample matrix [18].

To date the black-burnished earthenware fragments, each sample was divided into two parts. The first part was processed under subdued red light (640 ± 20 nm) to determine the AD, while the second part was prepared under ambient laboratory lighting to determine the D.

For AD determination, approximately 2 mm of material was removed from all surfaces of the fragments [19]. The sample was then ground using a mortar and pestle and sieved to obtain particles of approximately 90 μm in size. The quartz extraction process involved several chemical treatments. First, the sample was etched in 15% hydrochloric acid (HCl) for 40 min to remove carbonates and other acid-soluble impurities, followed by thorough rinsing with distilled water. Subsequently, the sample was treated with 35% hydrofluoric acid (HF) for 40 min to remove feldspars and to etch away the outer surface of quartz grains. After HF treatment, the samples were again rinsed with distilled water and then treated with 35% HCl for 15 min to eliminate any fluoride compounds formed during the HF process [20,21]. The samples were rinsed 3 time to 5 time with distilled water and dried at 50°C for 24 h. Heavy minerals, including metal ores, were removed using a magnetic separator.

For OSL measurement, stainless steel discs provided by Freiberg Instruments were coated with a 2 mm layer of silicone. Quartz grains were evenly sprinkled onto the discs, and non-adhering grains were gently removed by tapping the discs.

For the second part of the sample, this process focused on determining the concentration of natural radioisotopes—specifically uranium-238 (238U), thorium-232 (232Th), and potassium-40 (40K)—using laser ablation inductively coupled plasma mass spectrometry (LA-ICP-MS) (Thermo Fisher Scientific Inc., USA). These concentrations were used to calculate the annual dose (D) [22,23].

2.3 Accumulated dose and annual dose calculation

The AD was measured using the Lexygresearch TL/OSL Reader [24,25], equipped with a 90Sr/90Y beta source delivering a dose rate of 0.06 Gy·s^{-1} and a 525 nm green LED [26,27] and a 2.5 mm Hoya U-340 filter, at the Amata Siam Science Center in Bangkok, Thailand. The measurement was conducted using a modified version of the single aliquot regenerative (SAR) protocol [28,29].

Table 1. The OSL-SAR protocol used for AD determination.

Run	Operation
1	Give dose (N, R_1, R_2, R_3)
2	Preheat at 200°C (5°C·s^{-1}) for 50 s
3	OSL measurement (L_x)
4	Give Test dose
5	Cutheat at 125°C (5°C·s^{-1}) for 50 s
6	IRSL measurement, only last cycle
7	OSL measurement (T_x)
8	Return to run 1

For this study, preheating temperatures of 200°C followed by a cut-heat at 125°C was applied for AD determination. These temperatures were selected to effectively remove unstable signal components associated with shallow traps (via preheating), and to eliminate any unstable contributions from the test dose (via cut-heat), while preserving the stable electron traps responsible for the primary luminescence signal. The preheat temperature of 200°C is considered sufficient to empty thermally unstable traps without compromising the stability of the main dosimetric signal. This choice was based on prior studies and preliminary tests, which confirmed that 200°C effectively removes unstable signals related to shallow traps without affecting the stable luminescence signal integrity. Similarly, the cut-heat at 125°C ensures that residual signals from the test dose do not affect the subsequent measurement, a value chosen to balance signal removal and preservation of the stable traps.

Regarding the regenerative doses, we selected R_1 = 4.06 Gy, R_2 = 8.12 Gy, and R_3 = 12.18 Gy. These doses were determined based on dose recovery tests and sensitivity analyses, which showed that this range adequately covers the expected natural equivalent dose (De) values for our samples. This selection ensures a reliable growth curve construction while avoiding signal saturation or insufficient signal levels. A total of 15 aliquots were measured for each sample. The detailed SAR protocol employed in this study is presented in Table 1.

The D consists of four main components: the alpha dose (Dα), beta dose (Dβ), gamma dose (Dγ), and the cosmic dose (Dc). Dα, Dβ, and Dγ result from α-, β-, and γ-decays of the natural radioactive isotopes 238U, 232Th, and 40K. The Dc is also incorporated into the annual dose and is influenced by geographic characteristics including latitude, longitude, elevation, and is further attenuated by the burial depth of the sample [30]. In addition, radiation attenuation due to moisture within the sample matrix was accounted for. The water content was determined by calculating the difference between the sample's weight in its natural moist state and its oven-dried weight.

The contributions of radioactive elements to the total annual dose were calculated using the conversion factors provided by Adamiec and Aitken [31] , along with grain size attenuation factors described by Bell [32]. The Dc component was computed using the equations proposed by Prescott and Hutton [33]. The total annual dose and its associated uncertainty were calculated using the Dose Rate and Age Calculator (DRAC, version 1.2) [34] in combination with an error propagation formula.

2.4 Analysis of main component and firing temperature from XRD, EDS, and FE-SEM.

The analysis of the primary mineral components was conducted using an X-ray diffractometer (XRD), Bruker AXS Model D8 Advance (Germany), located at the Center of Scientific and Technological Equipment for Advanced Research, Thammasat University. Diffraction patterns were recorded at room temperature using Cu Kα radiation (λ = 1.5406 Å), with data collected over a 2θ range of 5° to 80° to identify the primary mineral phases present in the samples.

Morphological investigations were performed using a field emission scanning electron microscope (FE-SEM), JEOL JSM7800F (Japan), operated at an accelerating voltage of 15 kV. This instrument, also housed at the Center of Scientific and Technological Equipment for

Advanced Research, Thammasat University, was equipped with an energy-dispersive X-ray spectroscopy (EDS) system, Oxford X-Max 20 (United Kingdom), for elemental analysis based on X-rays emitted from the sample surface during SEM observation.

The firing temperature estimation was carried out by analyzing microstructural features observed in the SEM images [35]. These features provide insight into thermal alteration patterns resulting from the original firing processes of the samples.

3. Results and discussion

3.1 Mineralogical composition by XRD analysis

The X-ray diffraction (XRD) patterns of the earthenware samples, as shown in Figure 3, reveals that quartz is the dominant crystalline phase. The strongest diffraction peak appears at $2\theta \approx 26.6°$, corresponding to the (101) plane of quartz (JCPDS#46-1045). Additional peaks observed at $2\theta \approx 20.9°$, 36.5°, 39.5°, 50.1°, and 60.0° further confirm the presence of quartz with high crystallinity. Weak and broad peaks at other positions may indicate minor amounts of feldspar or clay minerals. Based on the relative intensity of the peaks, it is estimated that quartz accounts for approximately 85% to 90% of the crystalline phases [36,37].

This high quartz content is particularly significant for the application of optically stimulated luminescence (OSL) dating. Quartz is known for its reliable luminescence properties, and its dominance in the samples supports their suitability for luminescence signal measurement. These findings affirm that the samples are appropriate for OSL dating, which is the primary aim of this study.

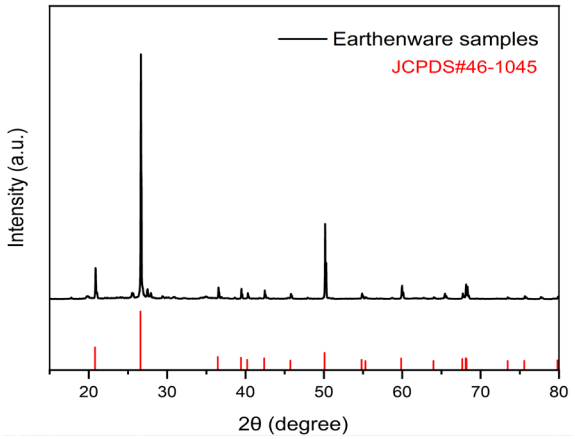

Figure 3. XRD patterns confirming quartz as the major phase in earthenware.

Table 2. Elemental concentrations of the earthenware sample from SEM-EDS analysis.

Element	Atomic weight %
C	15.01
O	59.37
Mg	0.66
Al	5.52
Si	16.17
Cl	0.49
K	1.05
Ca	0.75
Fe	0.98

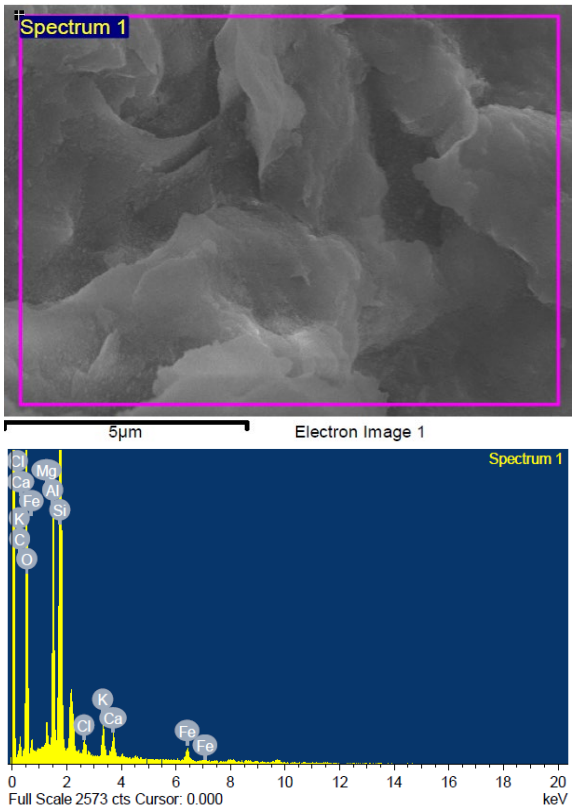

Figure 4. SEM photographs and EDS spectra of the earthenware sample.

3.2 Elemental composition by SEM–EDS

The elemental concentrations of the earthenware samples examined under scanning electron microscopy (SEM), together with energy dispersive X-ray spectroscopy (EDS), are presented in Table 2. The corresponding elemental mapping and EDS spectrum are shown in Figure 4. The EDS results indicate that oxygen and silicon are the dominant elements, with atomic percentages of approximately 59% and 16%, respectively. This distribution strongly suggests the presence of silica (SiO_2), as these two elements are the primary constituents of this compound [38,39].

The detection of only small amounts of other elements implies the presence of minor impurities or secondary mineral phases. Overall, the elemental composition is consistent with a silica-rich matrix, supporting the interpretation that quartz is the main crystalline phase. These findings align with the XRD results and further confirm the suitability of the samples for luminescence-based dating, particularly OSL.

3.3 Microstructural and compositional analysis for firing temperature estimation by SEM-EDS

Figure 5(a-c) show FE-SEM micrographs of the earthenware sample at magnifications of 5,000x, 10,000x, and 20,000x, respectively. The microstructure reveals a heterogeneous and partially sintered matrix with nanoscale porosity distributed throughout the material. The porous texture, along with limited glassy phases, indicates an incomplete vitrification process.

Embedded within the matrix are angular, subhedral to anhedral grains, which are characteristic of residual quartz (SiO_2) [40] that

has resisted melting during firing. These grains retain sharp edges and well-defined crystal boundaries, consistent with the high thermal stability of quartz, which typically remains solid up to temperatures around 1050°C [41,42].

The extent of vitrification observed is moderate. Some localized areas show partial glassy phase development, suggesting temperatures sufficient to initiate feldspar melting but insufficient for complete densification of the matrix. This degree of vitrification is characteristic of firing temperatures in the range of approximately 900°C to 1000°C [43].

This observation is consistent with the SEM-EDS results, which identify SiO_2 as the primary component, along with Al_2O_3, feldspar minerals ($KAlSi_3O_8$ and $CaAl_2Si_2O_8$), and minor traces of carbonates ($CaCO_3$).

Additionally, the detection of carbonates such as $CaCO_3$ indicates that the firing temperature was not excessively high, as these compounds generally begin to decompose between 800°C to 900°C [44]. The presence of undecomposed carbonate suggests that either the firing duration or atmospheric conditions during firing were insufficient for complete decomposition.

The FE-SEM micrographs (Figure 5) provide detailed insight into the microstructure of the earthenware sample at various magnifications. The images reveal preserved porosity distributed between the layered particles, particularly at higher magnifications, indicating incomplete densification. Microcracks are also visible along the particle boundaries, and localized vitrification—evidenced by partially fused grain surfaces—is present but not extensive. These features suggest that the firing process did not reach full vitrification, supporting the interpretation of a moderate firing regime. Taken together with the compositional analysis and the presence of residual quartz grains, this microstructural evidence indicates the use of traditional low-technology firing techniques, such as open firing or simple updraft kilns. These methods typically achieve peak temperatures close to, but rarely exceeding, 1000°C. Therefore, the firing temperature for this earthenware is estimated to be within the range of 900°C to 1000°C.

3.4 OSL results

The concentrations of uranium (238U), thorium (232Th), and potassium (40K) in the three earthenware samples were determined using LA-ICP-MS. The average values obtained were 6.78 ppm for uranium, 2.66 ppm for thorium, and 1.59% for potassium, as shown in Table 3.

These values are in reasonable agreement with the average concentrations found in the Earth's upper continental crust, which are approximately 2.8 ppm for uranium, 10.7 ppm for thorium, and 2.8% for potassium [45,46].

The slightly elevated uranium and lower thorium and potassium concentrations may reflect differences in clay source, firing conditions, and post-depositional alteration. Clay selection from uranium-rich deposits, loss of volatile elements during firing, and diagenetic processes such as groundwater interaction could account for the observed variation.

Overall, the elemental composition supports the interpretation that the raw materials were derived from natural crustal sources, with compositional deviations influenced by both technological practices and environmental factors after deposition.

The determination of the accumulated dose (AD) for each sample was achieved through a combined analysis of its OSL decay and growth curves.

Figure 6 displays the OSL decay curves following irradiation at 4.06 Gy, 8.12 Gy, and 12.18 Gy, alongside the natural signal. All decay curves exhibit the expected rapid decrease in OSL intensity with stimulation time, consistent with first-order kinetics characteristic of electron-hole recombination via optically stimulated pathways. A clear dose-dependent relationship is observed, with the initial OSL intensity scaling positively with the administered dose. The natural signal shows the lowest initial intensity, reflecting the limited number of charge carriers accumulated over geological timescales. In contrast, artificially irradiated aliquots demonstrate progressively higher initial intensities, proportional to the given dose, thereby confirming the fidelity of the trapping system and the absence of significant signal instability.

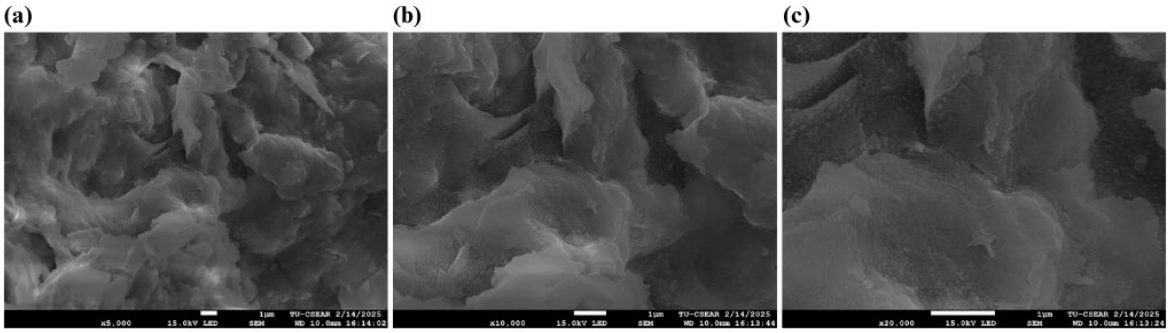

Figure 5. FE-SEM micrographs of the earthenware sample at different magnifications: (a) 5,000x, (b) 10,000x, and (c) 20,000x. The white scale bar in each image represents 1 μm.

Table 3. Concentration of 238U, 232Th, and 40K in the earthenware samples used to calculate the annual dose (D) of the samples.

Sample code	Concentration		
	238U [ppm]	**232Th [ppm]**	**40K [%]**
K1	6.68 ± 0.05	2.27 ± 0.39	1.27 ± 0.03
K2	6.79 ± 0.08	3.73 ± 0.65	1.66 ± 0.02
K3	6.87 ± 0.04	1.99 ± 0.51	1.85 ± 0.06

Table 4. Earthenware ages obtained using OSL method.

Sample code	AD [Gy]	D [mGy·a^{-1}]	OSL Age [ka]
K1	9.59 ± 0.41	2.67 ± 0.46	3.591 ± 0.63
K2	9.71 ± 0.38	2.79 ± 0.58	3.479 ± 0.74
K3	10.15 ± 0.51	2.73 ± 0.52	3.717 ± 0.73

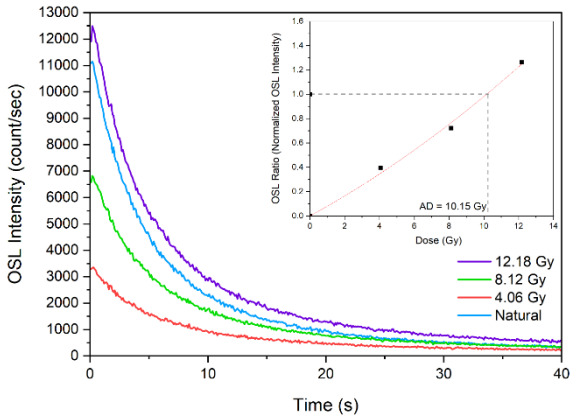

Figure 6. OSL decay curve of the K3 sample for both natural and laboratory doses. The inset shows the OSL growth curve of the K3 sample, illustrating the estimated accumulated dose.

The OSL growth curve for the K3 sample, shown in the inset of Figure 6, further elucidates the dose-response behavior. The normalized OSL intensity increases with dose, following a characteristic saturating exponential function [47], which reflects the finite number of available trapping sites [48]. The fitted growth curve closely matches the experimental data points (black squares), underscoring the robustness of the dose calibration. The natural OSL signal projects onto this curve at an accumulated dose (AD) of 10.15 Gy, as indicated by the intersection of the dashed lines.

The consistent behavior observed in both the OSL decay and growth analyses reinforces the reliability of the estimated AD. The well-defined growth curve, together with the systematic decay characteristics, suggests minimal influence from unstable or non-reproducible trapping centers. These findings indicate that the K3 sample is well-suited for accurate dose reconstruction and, consequently, for reliable age determination.

The age of all samples was calculated by dividing the accumulated dose (AD) by the annual dose rate (D), as shown in Table 4. The mean OSL age of 3.59 ± 0.70 ka places the samples within the Late Neolithic to Middle–Late Bronze Age. These ages align well with estimations obtained from the online dose rate and age calculator for quartz, using standard dose conversion factors. Additionally, the OSL-derived ages are consistent with the typological features of the earthenware and radiocarbon dates of artifacts linked to the Ban Kao cultural complex in Kanchanaburi Province, Thailand—an archaeological tradition dated to approximately 3,000 to 4,000 years ago. This concordance supports the proposed chronological framework and demonstrates the reliability of OSL dating for archaeological ceramics in the region.

4. Conclusions

This study successfully applied optically stimulated luminescence (OSL) dating to determine the age of black-burnished earthenware fragments from the Nam Tok Khao Pang archaeological site in Kanchanaburi province, Thailand. Mineralogical analysis confirmed quartz (SiO_2) as the major phase through XRD patterns, further supported by EDS and SEM observations revealing a partially sintered silicate matrix with impurities and an absence of vitrification, indicating firing temperatures between 900°C and 1000°C. The annual dose rates, derived from U, Th, and K concentrations analyzed via LA-ICP-MS, ranged from 2.67 ± 0.46 mGy·a^{-1} to 2.79 ± 0.58 mGy·a^{-1}, while the accumulated doses obtained from OSL measurements varied from 9.59 ± 0.41 Gy to 10.15 ± 0.51 Gy. These data yielded an average age of 3.59 ± 0.70 ka, placing the artifacts in the Late Neolithic to Middle–Late Bronze Age. The results align well with typological characteristics and radiocarbon data from the Ban Kao cultural complex, reinforcing regional chronological frameworks and demonstrating the effectiveness of OSL dating for ceramics in tropical contexts.

Future research could extend this integrative approach to other sites in mainland Southeast Asia, contributing to a comparative framework that illuminates broader patterns of cultural interaction, ceramic technology, and settlement dynamics during the Late Neolithic to Bronze Age.

Acknowledgements

The authors gratefully acknowledge the Museum and Prehistoric Laboratory, Sud Saengvichien (Siriraj Museum), for kindly providing the samples used in this study. The authors also wish to express their profound gratitude to the Amata Siam Science Center (ASSC) for its invaluable financial support and for providing access to critical research facilities, including the Lexygresearch TL/OSL Reader and the laser ablation inductively coupled plasma mass spectrometry (LA-ICP-MS) system. The contributions of both institutions were essential to the successful completion of this research.

References

[1] P. Sorensen, “Preliminary report on the investigations of the Thai- Danish prehistoric expedition 1960-62 in the hamlet of Ban Kao, Kanchanaburi Province, Thailand,” 1960.

[2] C. Higham, T. Higham, R. Ciarla, K. Douka, A. Kijngam, and F. Rispoli, “The origins of the bronze age of Southeast Asia,” *Journal of World Prehistory*, vol. 24, no. 4, pp. 227–274, 2011.

[3] P. Thammapreechakorn, “Southeast Asian Ceramics Museum Newsletter,” 2016.

[4] D. Bayard, and R. H. Parker, “Commentary interpretation of Sai Yok and Ban Kao Sites, Central Thailand,” *Asian Perpectives*, vol. 19, no. 2, pp. 289-294, 1976.

[5] P. Sorensen, and T. Hatting, “Archaeological excavations in Thailand. Vol. II. Ban Kao: Neolithic settlements with cemeteries in the Kanchanaburi Province. Part I: The archaeological material

from the burials. The Thai-Danish Prehistoric Expedition 1960–1962.," Copenhagen: Munksgaard., 1967.

[6] J. K. Feathers, "Methods and applications in trapped charge dating," *Methods and Protocols*, vol. 24, no. 3, pp. 1–3, 2020.

[7] M. J. Aitken, P. Trans Roy, and B. M. J Aitken, "Dating by archaeomagnetic and thermoluminescent methods," 1970.

[8] M. J. Aitken, "Thermoluminescence dating of ancient pottery," *Nature*, vol. 219, no. 3, pp. 442–445, 1968.

[9] J. Wallinga, A. S. Murray, A. G. Wintle, and L. Bøtter-Jensen, "Electron-trapping probability in natural dosemeters as a function of irradiation temperature," Nuclear Technology Publishing, 2002.

[10] L. Janz, J. K. Feathers, and G. S. Burr, "Dating surface assemblages using pottery and eggshell: Assessing radiocarbon and luminescence techniques in Northeast Asia," *Journal of Archaeological Science*, vol. 57, pp. 119–129, 2015.

[11] J. Wei, J. Jin, L. Fu, X. Zuo, J. Qiu, C. Hou, and D. Xu,"New chronology evidence of prehistoric human activities indicated by pottery luminescence dating in the humid subtropical mountains of South China Journal of Archaeological Science, vol. 171, p. 106072, 2024.

[12] F. Preusser, D. Degering, M. Fuchs, A. Higers, A. Kadereit, N. Klasen, M. Krbetschek, D. Richter, and J. Q. G. Spencer, "Luminescence dating: basics, methods and applications," *E&G Quaternary Science Journa*, vol. 57, pp. 95-149, 2008.

[13] J. A. Durcan, "Luminescence dating," in Encyclopedia of Geology: Volume 1-6, Sec-ond Edition, Elsevier, 2020, pp. 164–174.

[14] M. J. Aitken, Science-based dating in archaeology. Routledge, 2013.

[15] H. van Es, "Thermoluminescence dating of sediments using mineral zircon," 2008. [Online]. Available: http://www.rug.nl/research/portal.

[16] I. Liritzis, A. K. Singhvi, J. K. Feathers, G. A. Wagner, A. Kadereit, N. Zacharias, and S. Li, "Luminescence Dating of Archaeological Materials," in Luminescence Dating in Archaeology, Anthropology, and Geoarchaeology, 2013, pp. 25–40. .

[17] S. A. Mahan, T. M. Rittenour, M. S. Nelson, N. Ataee, N. Brown, R. DeWitt, J. Durcan, M. Evans, J. Feathers, M. Frouin, G. Guerin, M. Heydari, S. Huot, M. Jain, A. Keen-Zebert, B. Li, G. I. Lopez, C. Neudorf, N. Porat, K. Rodrigues, A. Sawakuchi, J. Q. G. Spencer, and K. J. Thomsen, "Guide for interpreting and reporting luminescence dating re-sults," *Geological Society of America Bulletin*, vol. 135, no. 5–6, pp. 1480–1502, 2023.

[18] A. Doménech-Carbó, "Dating: an analytical task," *ChemTexts*, vol. 1, no. 1, 2015.

[19] S. Pailoplee, B. Chaisuwan, I. Takashima, K. Won-In, and P. Charusiri, "Dating ancient remains by thermoluminescence: Impli-cations of incompletely burnt bricks," *Bulletin of earth sciences of Thailand*, vol. 3, no. 1, pp. 8-16, 2010.

[20] D. R. G. Tudela et al., "TL, OSL and C-14 Dating Results of the Sediments and Bricks from Mummified Nuns' Grave," 2012. [Online]. Available: www.scielo.br/aabc

[21] A. Avram, D. Constantin, Q. Hao, and A. Timar-Gabor, "Optically stimulated lumi-nescence dating of loess in South-Eastern China using quartz and polymineral fine grains," *Quat Geochronol*, vol. 67, 2022.

[22] C. N. de Carvalho, F. Muñiz, L. M. Cáceres, J. Rodríguez-Vidal, A. Medialdea, M. del Val, P. P. Cunha, J. M. García, F. Giles-Guzmán, J. S. Carrión, Z. Belaústegui, A. Toscano, P. Gómez, J. M. Galán, J. Belo, M. Cachão, F. Ruiz, S. Ramirez-Cruzado, G. Finlayson, S. Finlayson, and C. Finlayson, "Neanderthal footprints in the 'Matalascañas trampled sur-face' (SW Spain): new OSL dating and Mousterian lithic industry," *Quaternary Science Reviews*, vol. 313, p. 108200, 2023.

[23] Y. J. Jeong, M. J. Jung, U. S. Ahn, and A. C. sik Cheong, "Laser ablation MC-ICPMS U-Th and U-Th-Pb dating of Quaternary zircons from Jeju Island, Korea," *Journal of Analytical Science and Technology*, vol. 15, no. 1, 2024.

[24] D. Richter, A. Richter, and K. Dornich, "Lexsyg - A new system for luminescence re-search," *Geochronometria*, vol. 40, no. 4, pp. 220–228, 2013.

[25] J. Sanjurjo-Sánchez, C. Arce-Chamorro, J. R. Vidal-Romaní, and N. Matin, "OSL da-ting of very young aeolian sediments of NW Spain to assess dune erosion and accre-tion periods," *Quaternary Geochronology*, vol. 82, 2024.

[26] L. Ageby, J. Shanmugavel, M. Jain, A. S. Murray, and E. F. Rades, "Towards the op-tically stimulated luminescence dating of unheated flint," *Quaternary Geochronology*, vol. 79, 2024.

[27] S. Bate, T. Stevens, J. P. Buylaert, S. B. Marković, P. Roos, and N. Tasić, "Pottery versus sediment: Optically stimulated luminescence dating of the Neolithic Vinča culture, Serbia," *Quaternary International*, vol. 429, pp. 45–53, 2017.

[28] A. S. Murray, and A. G. Wintle, "The single aliquot regenerative dose protocol: Poten-tial for improvements in reliability," in *Radiation Measurements*, vol. 37, no. 4-5, pp. 377–381, 2003.

[29] J. A. Durcan, and G. A. T. Duller, "Further investigation of spatially resolved single grain quartz OSL and TL signals," *Radiation Measurements,* vol. 177, p. 107260, 2024.

[30] G. Guérin, C. Christophe, A. Philippe, A. S. Murray, K. J. Thomsen, C. Tribolo, P. Urbanova, M. Jain, P. Guibert, N. Mercier, S. Kreutzer, and C. Lahaye, "Absorbed dose, equivalent dose, measured dose rates, and implica-tions for OSL age estimates: Introducing the Average Dose Model," *Quaternary Geochronology*, vol. 41, pp. 163–173, 2017.

[31] G. Guérin, N. Mercier, G. Adamiec, G. Guérin, N. Mercier, and G. Adamiec, "Dose-rate conversion factors: Update," *Ancient TL*, vol. 29, no. 1, pp. 5–8, 2011.

[32] W. T. Bell, "Thermoluminescence dating: Radiation dose-rate data.," *Archoeornerry*, vol. 21, pp. 243–245, 1979.

[33] J. R. Prescott, and J. T. Hutton, "Cosmic ray contributions to dose rates for lumines-cence and ESR dating: Large depths and long-term time variations," *Radiation Measurements*, vol. 23, no. 2-3, pp. 497-500, 1994.

[34] J. A. Durcan, G. E. King, and G. A. T. Duller, "DRAC: Dose Rate and Age Calculator for trapped charge dating," *Quaternary Geochronology*, vol. 28, pp. 54–61, 2015.

[35] M. S. Tite, "The Impact of Electron Microscopy on Ceramic Studies," *The British Aceadmay*, pp. 111-113, 1991.

[36] P. H. Ribbe, C. Prewitt, and G. V. Gibbs, "Physical behavior, geochemistry, and materials applications," *Silica*, vol. 29. Peter J. Heaney, Princeton, New Jersey, USA, 1994.

[37] C. Zhang, Z. Xu, Y. Hu, J. He, M. Tian, J. Zhou, Q. Zhou, S. Chen, D. Chen, P. Chen, and W. Sun, "Novel insights into the hydroxylation behaviors of α-quartz (101) surface and its effects on the adsorption of sodium oleate," *Minerals*, vol. 9, no. 7, p. 450, 2019.

[38] I. M. Joni, L. Nulhakim, M. Vanitha, and C. Panatarani, "Characteristics of crystalline silica (SiO_2) particles prepared by simple solution method using sodium silicate (Na_2SiO_3) precursor," *Journal of Physics: Conference Series*, vol. 1080, no. 1, p. 012006, 2018.

[39] A. Bintintan, M. Gligor, I. D. Dulama, S. Teodorescu, R. M. Stirbescu, and C. Rad-ulescu, "ATR-FTIR and SEM-EDS analyses of lumea noua painted pottery from Alba Iulia-Lumea Noua Neolithic site," *Revista de Chimie*, vol. 68, no. 4, pp. 847–852, 2017.

[40] B. Das, and J. K. Mohanty, "Mineralogical characterization and beneficiation studies of pyrophyllite from orissa, India." *Journal of Minerals and Materials Characterization and Engineering*, vol. 8 , no. 4, pp. 329-338, 2009.

[41] G. Lalle, E. Rossi, M. Sebastiani, F. Sarasini, and J. Tirillò, "Effect of medium-high temperature conditioning on the mechanical properties of single quartz fibres," *Journal of the European Ceramic Society*, vol. 43, no. 16, pp. 7599–7612, 2023.

[42] I. Giannopoulou, P. M. Robert, K. M. Sakkas, M. F. Petrou, and D. Nicolaides, "High temperature performance of geopolymers based on construction and demolition waste," *Journal of Building Engineering*, vol. 72, 2023.

[43] M. S. Tite, I. Freestone, N. Meeks, and M. Bimson, "The use of scanning electron microscopy in the technological examination of ancient ceramics," in book *Archaeological Ceramics*, Smithsonian Institution PressEditors: J S Olin and A D Franklin, 1982, pp.109-120.

[44] D. Zhuang, Z. Chen, and B. Sun, "Thermal decomposition of calcium carbonate at multiple heating rates in different atmospheres using the techniques of TG, DTG, and DSC," *Crystals (Basel)*, vol. 15, no. 2, 2025.

[45] M. Javoy, and E. Kaminski, "Earth's uranium and thorium content and geoneutrinos fluxes based on enstatite chondrites," *Earth and Planetary Science Letters*, vol. 407, pp. 1–8, 2014.

[46] M. Tzortzis, and H. Tsertos, "Determination of thorium, uranium and potassium ele-mental concentrations in surface soils in Cyprus," *Journal of Environmental Radioactivity*, vol. 77, no. 3, pp. 325–338, 2004.

[47] Y. J. Guo, B. Li, J. F. Zhang, B. Y. Yuan, F. Xie, and R. G. Roberts, "New ages for the upper palaeolithic site of Xibaimaying in the Nihewan Basin, northern China: Impli-cations for small-tool and microblade industries in north-east Asia during Marine Iso-tope Stages 2 and 3," *Journal of Quaternary Science*, vol. 32, no. 4, pp. 540–552, 2017.

[48] A. S. Murray, J. M. Olley, and A. S. Murray, "Precision and accuracy in the optically stimulated luminescence dating of sedimentary quartz: A status review," *Geochronometria*, vol. 21, 2002.